Journal of Medicinal Chemistry

Article

pubs.acs.org/jmc

Bivalent Smac Mimetics with a Diazabicyclic Core as Highly Potent Antagonists of XIAP and cIAP1/2 and Novel Anticancer Agents

Yuefeng Peng,[‡,†] Haiying Sun,[†] Jianfeng Lu, Liu Liu, Qian Cai,[§] Rong Shen,[∥] Chao-Yie Yang, Han Yi, and Shaomeng Wang*

Comprehensive Cancer Center and Departments of Internal Medicine, Pharmacology, and Medicinal Chemistry, University of Michigan, 1500 E. Medical Center Drive, Ann Arbor, Michigan 48109, United States

ABSTRACT: Nonpeptidic, bivalent Smac mimetics designed based upon monovalent Smac mimetics with a diazabicyclic core structure bind to XIAP, cIAP1, and cIAP2 with low to subnanomolar affinities and are highly effective in antagonizing XIAP in cell-free functional assays. They efficiently induce the degradation of cIAP1 and cIAP2 in cancer cells at concentrations as low as 1 nM, activate caspase-3 and -8, and cleave PARP at 3−10 nM. The most potent compounds in the series have IC_{50} of 3−5 nM in inhibition of cell growth in both MDA-MB-231and SK-OV-3 cell lines and are promising lead compounds for the development of a new class of cancer therapy.

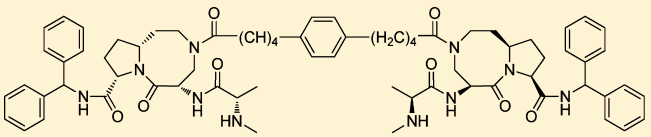

A New Class of Highly Potent XIAP and cIAP1/2 Inhibitors

INTRODUCTION

Apoptosis, or programmed cell death, is a cell process critical for homeostasis, normal development, host defense, and suppression of oncogenesis. Faulty regulation of apoptosis has been implicated in many human diseases,[1] including cancer,[2,3] and it is now recognized that resistance to apoptosis is a hallmark of cancer.[4] As a consequence, targeting of key apoptosis regulators has emerged as an attractive strategy for the development of new approaches to human cancer treatment.[1]

Although their roles are not limited to regulation of apoptosis,[7,8] inhibitors of apoptotic proteins (IAP) are a class of key apoptosis regulators and are characterized by the presence of one or more BIR (baculoviral IAP repeat) domains.[5,6] Among the IAPs, cellular IAP1 (cIAP1) and cIAP2 play a key role in the regulation of death-receptor mediated apoptosis, whereas X-linked IAP (XIAP) inhibits both death-receptor mediated and mitochondria mediated apoptosis by binding to and inhibiting caspase-3/7 and caspase-9, three cysteine proteases critical for execution of apoptosis.[5] These IAP proteins are highly overexpressed both in cancer cell lines and in human tumor tissues and have low expression in normal cells and tissues.[9] Extensive studies have demonstrated that overexpression of IAP proteins makes cancer cells resistant to apoptosis induction by a variety of anticancer drugs.[10−12] Hence, targeting one or more of these IAP proteins is thought to be a novel and promising therapeutic strategy for the treatment of human cancer.[10−13]

RESULTS AND DISCUSSION

Smac/DIABLO (second mitochondria-derived activator of caspases or direct IAP binding protein with low pI) is a protein released from mitochondria in response to apoptotic stimuli and functions as an endogenous inhibitor of cIAP1, cIAP2, and XIAP.[14,15] The interaction between Smac and IAPs is mediated by the N-terminal AVPI tetrapeptide motif in Smac and one or more BIR domains in these IAP proteins.[16,17] Smac is a homodimer that binds to both the BIR2 and BIR3 domains in XIAP and antagonizes the inhibition of XIAP to caspase-3/-7 and caspase-9.[18] In comparison, Smac binds to only the BIR3 domain in cIAP1 and cIAP2[19] and induces the proteins' rapid degradation in cells.[20] Through two distinct mechanisms, Smac is a very efficient antagonist of these three IAP proteins.

The crystal and NMR structures of XIAP BIR3 complexed with Smac protein or Smac peptide show that the AVPI tetrapeptide motif in Smac binds to a well-defined surface groove in XIAP, and this interaction represents an attractive site for the design of small-molecule XIAP inhibitors.[16−18] By use of AVPI tetrapeptide as the lead structure, several classes of small-molecule Smac mimetics have been designed as antagonists of XIAP and cIAP1/2.[21−38] Two different types of Smac mimetics have been designed.[21−23] The first type, designed to mimic a single AVPI binding motif, is called monovalent Smac mimetics.[21−23] The second type, the bivalent Smac mimetics, consists of two AVPI mimetics, tethered through a linker, to mimic the dimeric form of Smac proteins.[21−23] One key advantage for monovalent Smac mimetics as potential drugs is that they can achieve oral bioavailability, but a drawback is that they only have modest potency in antagonizing full-length XIAP in functional assays. A major advantage of bivalent Smac mimetics is that they are much more potent antagonists of XIAP than monovalent Smac mimetics by concurrently targeting both BIR2 and BIR3 domains in XIAP.[30] Bivalent Smac mimetics

Received: August 10, 2011
Published: December 7, 2011

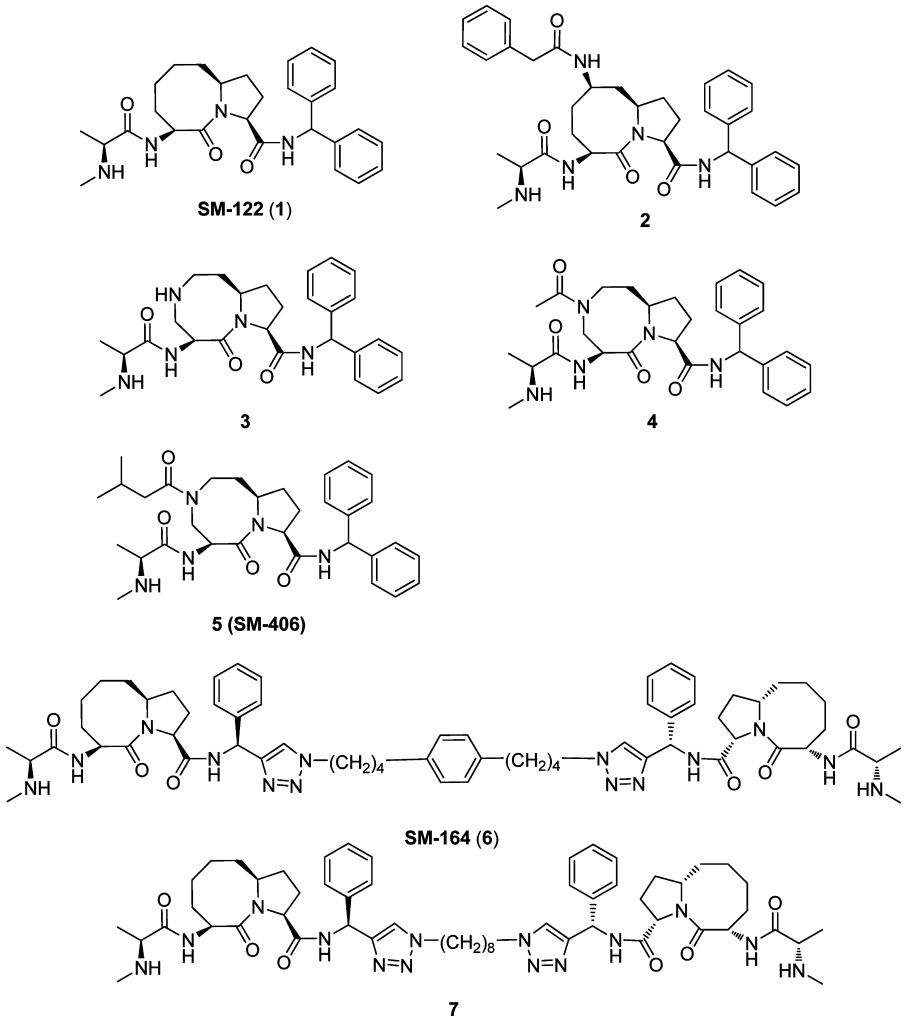

Figure 1. Chemical structures of representative Smac mimetics reported by our laboratory. Compounds **1**−**5** are monovalent Smac mimetics, and compounds **6** and **7** are bivalent Smac mimetics.

Table 1. Binding Affinities of Newly Designed Smac Mimetics to XIAP L-BIR2-BIR3, cIAP1 BIR3, cIAP2 BIR3, XIAP BIR3, and XIAP BIR3 Proteins, As Determined in Fluorescence-Polarization Assays[a]

	XIAP L-BIR2-BIR3		cIAP1 BIR3		cIAP2 BIR3		XIAP BIR3		XIAP BIR2	
compd	IC_{50} (nM)	K_i (nM)	IC_{50} (nM)	K_i (nM)	IC_{50} (nM)	K_i (nM)	IC_{50} (nM)	K_i (nM)	IC_{50} (μM)	K_i (μM)
1	1240 ± 42	408 ± 14	46.2 ± 8.3	6.7 ± 1.2	74.7 ± 12.1	18.3 ± 2.9	636 ± 51	191 ± 15	18.9 ± 4.0	8.2 ± 1.5
4	169 ± 28	51 ± 9	7.6 ± 0.1	1.1 ± 0.1	14.5 ± 2.5	3.0 ± 0.7	208 ± 18	70 ± 6	14.3 ± 1.1	5.5 ± 0.5
6	7.5 ± 0.8	2 ± 0.2[b]	4.6 ± 0.7	0.5 ± 0.1	8.5 ± 4.2	2.0 ± 1.0	153 ± 5	45 ± 2		
7	6.4 ± 2.7	2 ± 1[b]	2.8 ± 0.8	<0.5[b]	8.2 ± 1.9	2 ± 0.4	134 ± 11	39 ± 3		
8	13.7 ± 3.8	3 ± 1[b]	6.1 ± 0.7	0.7 ± 0.1	9.9 ± 0.6	1.7 ± 0.2	188 ± 37	63 ± 13		
9	7.6 ± 0.3	2 ± 0.1[b]	4.5 ± 0.4	0.4 ± 0.1	8.2 ± 1.0	1.3 ± 0.3	145 ± 19	48 ± 7		
10	7.8 ± 2.0	2 ± 0.4[b]	8.6 ± 1.6	1.2 ± 0.3	15 ± 3	3.3 ± 0.7	161 ± 23	54 ± 8		
11	10.0 ± 1.3	2 ± 0.3[b]	12.9 ± 1.9	2.0 ± 0.4	27 ± 4	6.4 ± 1.1	217 ± 11	73 ± 4	4.3 ± 0.5	1.1 ± 0.2
12	17.7 ± 1.7	3 ± 0.3[b]	12.4 ± 2.6	1.9 ± 0.5	29 ± 4	6.9 ± 1.2	289 ± 39	98 ± 13		
13	11.5 ± 3.2	2 ± 0.6[b]	17.4 ± 1.9	2.9 ± 0.4	52 ± 6	14 ± 2	311 ± 43	106 ± 15	9.4 ± 0.1	3.4 ± 0.1
14	6.3 ± 1.3	1 ± 0.2[b]	8.5 ± 2.2	1.2 ± 0.4	18 ± 2	4.0 ± 0.5	203 ± 22	68 ± 8		
15	24.0 ± 13	5 ± 2[b]	21.2 ± 1.7	3.6 ± 0.3	43 ± 5	11 ± 1	715 ± 114	246 ± 39		

[a]Compounds **1**, **4**, **6**, and **7** were included as control compounds for comparison. [b]Exceeded lower assay limits: K_i values are estimated.

are typically 2−3 orders of magnitude more potent than their monovalent Smac mimetic counterparts in induction of apoptosis in cancer cells.[21]

Currently, three monovalent and two bivalent Smac mimetics have been advanced into clinical trials for the treatment of human cancer.[21] A number of representative monovalent and bivalent Smac mimetics designed by our laboratory are shown in Figure 1. Compound **5** (AT-406), an orally active Smac mimetic, is currently in phase I clinical trials for the treatment of solid tumors and leukemia.[37]

dx.doi.org/10.1021/jm201072x | J. Med. Chem. 2012, 55, 106−114

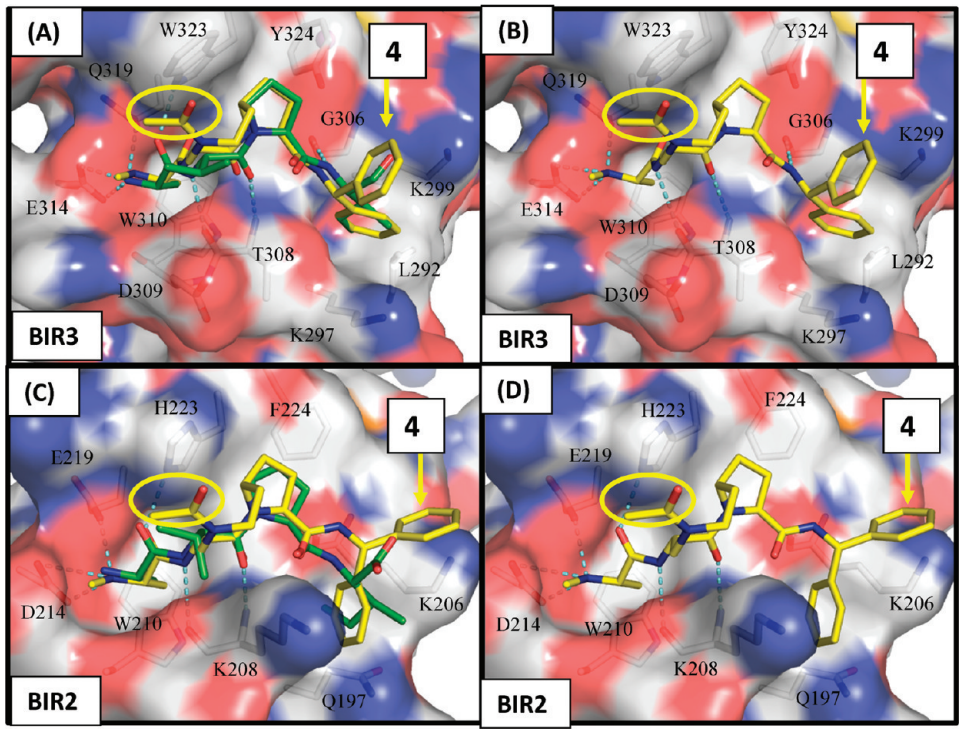

Figure 2. Predicted binding models of compound **4** in complex with XIAP (A, B) BIR3 and (C, D) BIR2. The crystal structure of Smac AVPI peptide (green color) in complex with XIAP BIR3 and the predicted binding model of the same peptide with BIR2 are superimposed in (A) and (C), respectively. Key residues around the binding site are shown and labeled. The dimer linkage sites in compound **4** are circled in yellow.

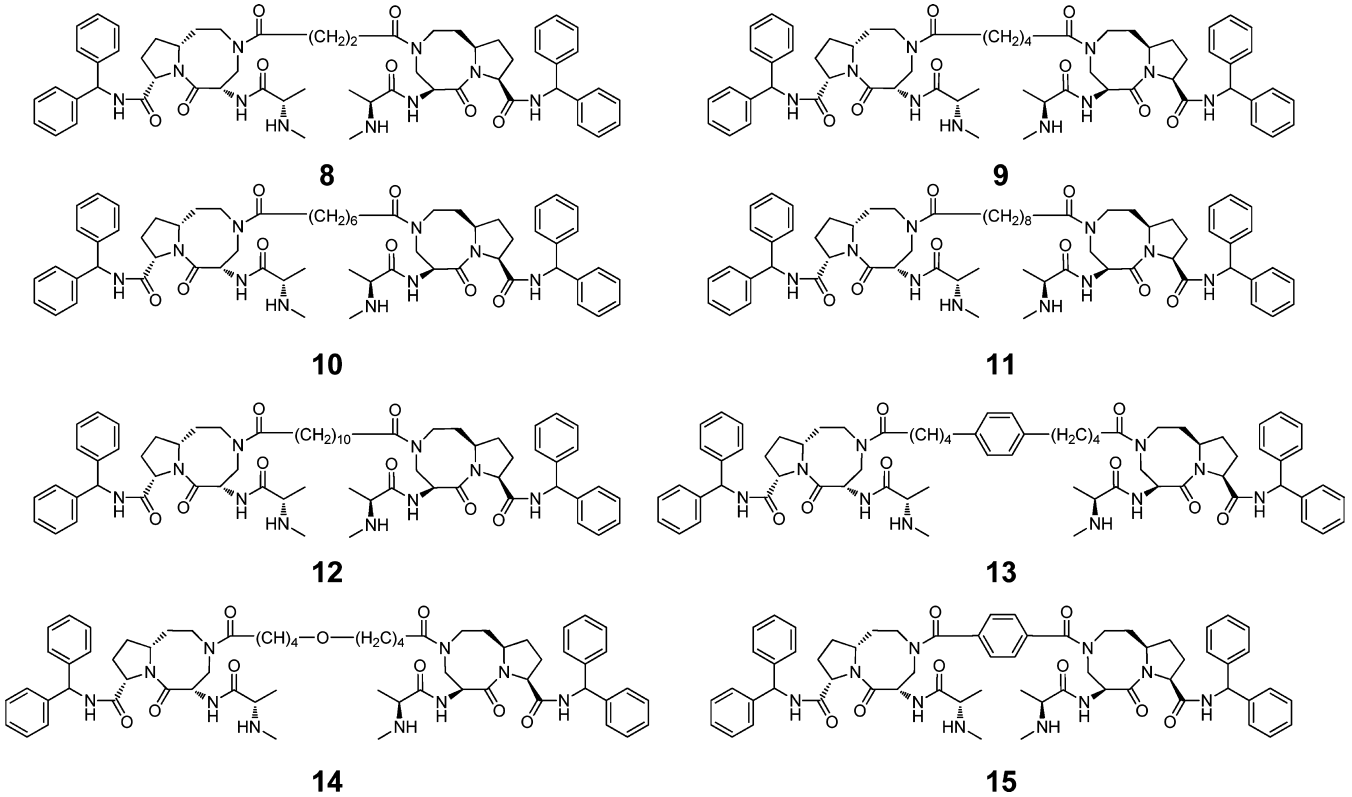

Figure 3. Chemical structures of designed new bivalent Smac mimetics based upon the core structure of monovalent Smac mimetics **4** and **5**.

Since bivalent Smac mimetics are much more potent than monovalent Smac mimetics in targeting XIAP and cIAP1/2 and in induction of apoptosis of cancer cells in vitro and in vivo and in inhibition of tumor growth, we have pursued the design and development of such compounds for cancer treatment.[21] In earlier studies,[30,31,38] we reported the design of a series of bivalent Smac mimetics, exemplified by compounds **6** and **7**, based upon the core structure of monovalent Smac mimetic **1**.

dx.doi.org/10.1021/jm201072x | J. Med. Chem. 2012, 55, 106–114

In the present study, we report the design, synthesis, and evaluation of a new class of bivalent Smac mimetics containing a diazabicyclic core structure contained in monovalent Smac mimetics **4**–**6**, which have a favorable pharmacokimetic (PK) and toxicity profile. For example, compound **5** (SM-406/AT-406) demonstrates an excellent PK and toxicity profile in rodents and non-rodents and is now in clinical trials for cancer treatment.[37] Therefore, we have sought to design new classes of bivalent Smac mimetics based upon the core structure in compounds **4**–**6**.

For the design of bivalent Smac mimetics, three key issues need to be considered. The first is the identification of a suitable monovalent Smac mimetic, which can bind to both the BIR2 and BIR3 domains of XIAP with good affinities. The second issue is the identification of a suitable tethering site, and the third is the determination of optimal length and properties of the linker used to tether two monovalent mimetics. In our previous study,[38] we have shown that the linker has a major effect on the overall cellular activity of the designed bivalent Smac mimetics by modulation of their cell permeability, although it has a minimal effect on the biochemical binding to XIAP, cIAP1, and cIAP2.

In our binding assays, compound **4** binds to XIAP BIR3 with K_i = 51 nM and to XIAP BIR2 with K_i = 5.5 μM (Table 1). Since compound **4** has good affinities to both BIR3 and BIR2 domains in XIAP, it represents an excellent monovalent lead compound for the design of new bivalent Smac mimetics with the objective to currently target both BIR2 and BIR3 domains in XIAP. To identify suitable sites for tethering, we modeled **4** in a complex with the BIR2 and BIR3 domains of XIAP (Figure 2). These models revealed that the amide group in the eight-membered ring being exposed to solvent (Figure 2) is a suitable site for tethering. Accordingly, we designed a series of bivalent Smac mimetics (**8**–**15**) by linking two molecules of compound **4** through this site (Figure 3). The synthesis of these compounds is shown in Scheme 1.

Scheme 1. Synthesis of Bivalent Smac Mimetics 8–15[a]

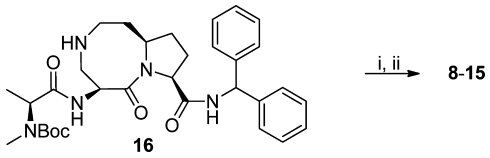

[a]Reagents and conditions: (i) diacyl chloride, *N*,*N*-diisopropylethylamine, CH_2Cl_2; (ii) 4 N HCl, 1,4-dioxane, methanol.

Compounds **8**–**12** were designed to have a linear, flexible alkane linker with different lengths, from 2 carbon atoms (**8**) to 10 carbon atoms (**12**), in order to investigate the influence of the linker length on binding affinities to IAP proteins and cellular activities. In our fluorescence-polarization-based (FP-based) binding assay,[38] compounds **8**–**12** have similar high affinities to XIAP protein containing both BIR2 and BIR3 domains, with IC_{50} ranging from 7.6 to 17.7 nM and calculated K_i of 2–3 nM (Table 1). Their binding affinities to XIAP BIR2-BIR3 protein exceed the lower limits of the assay, and so their K_i values are underestimated. Our previous study has shown that the bivalent Smac mimetic **6** achieves a much higher affinity to XIAP containing both BIR2 and BIR3 domains than its corresponding monovalent counterparts by concurrently binding to both BIR domains.[30] To investigate this aspect, we evaluated their binding affinities to XIAP protein containing only the BIR3 domain or BIR2 domain (Table 1). Our data showed that compounds **8**–**12** bind to XIAP BIR3 protein with IC_{50} of 145–289 nM and K_i of 48–98 nM, very similar to those for compounds **6** and **7**. Compounds **11** and **13** bind to XIAP BIR2 protein with K_i of 1.1 and 3.4 μM, respectively (Table 1). Therefore, these new bivalent Smac mimetics bind to XIAP protein containing both BIR2 and BIR3 domains with affinities >20 times higher than to XIAP BIR3 protein and >100 times higher than to XIAP BIR2 proteins. Hence, consistent with our previous study for compound **6**,[30] these data suggest that this new class of bivalent Smac mimetics achieves a much higher affinity to XIAP BIR2-BIR3 proteins than to XIAP BIR2 and BIR3 proteins by concurrently binding to both BIR domains in XIAP. Furthermore, the very similar high binding affinities to XIAP BIR2-BIR3 protein between these new bivalent Smac mimetics suggest that the region between BIR2 and BIR3 domains in XIAP is flexible and the protein can readily adopt a conformation for concurrently and efficiently binding to both of the AVPI mimetics in these bivalent Smac mimetics.

Compounds **8**–**12** also bind to cIAP1 BIR3 protein with high affinities, with IC_{50} of 4.5–12.9 nM and K_i of 0.4–2.0 nM (Table 1). They also have high affinities for cIAP2 BIR3 protein with IC_{50} of 8.2–29 nM and K_i of 1.3–6.9 nM, a 4-fold difference (Table 1). Compound **9** with a four-carbon linker appears to have the highest binding affinities to these three IAP proteins. These data show that the length of the linker in this class of bivalent Smac mimetics has only a modest effect on binding affinities to all three IAP proteins. Furthermore, the binding affinities of these new, bivalent Smac mimetics to cIAP1 and cIAP2 proteins are also similar to those of the corresponding monovalent Smac mimetic **4** (Table 1).

To investigate if the nature of the linker has a significant effect on binding to the three IAP proteins, we synthesized compounds **13**, **14**, and **15**. The linker in **13** has a length similar to that in **12** but is less flexible because of the presence of the phenyl group in its linker. Compound **13** binds to XIAP BIR2-BIR3, cIAP1, and cIAP2 proteins with K_i values of 2.0, 2.9, and 14 nM, respectively, very similar to those for **12**. Hence, we concluded that the conformational restriction by the phenyl group has no significant effect on binding affinities to these IAP proteins. Compound **14**, in which an oxygen atom is inserted into the linker in compound **11**, has K_i values of 1.0, 1.2, and 4.0 nM to XIAP, cIAP1, and cIAP2, respectively, and thus is slightly more potent than **11**. Compound **15**, in which a phenyl ring was used in the linker, has K_i values of 5.0, 3.6, and 11 nM to XIAP, cIAP1, and cIAP2, respectively. Compounds **15** and **9** have similar linker lengths, but **15** is several times less potent than **9** in binding to the three IAP proteins. Since the linker in **15** is much more conformationally rigid than the linker in **9**, the binding data indicate that a short, rigid linker is not optimal for binding to these IAP proteins in this class of compounds.

XIAP functions as a potent inhibitor of caspase-3 and caspase-9,[18] and dimeric Smac protein antagonizes XIAP by binding concurrently to both the BIR2 and BIR3 domains.[30] We thus evaluated the functional antagonism of these bivalent Smac mimetics in in vitro functional assays. Since XIAP binds to and antagonizes caspase-3 using its BIR2 domain, together with the immediate linker preceding BIR2, and binds to and antagonizes caspase-9 through its BIR3 domain, we used an XIAP construct containing linker-BIR2-BIR3 domain (residues 120–356) in our functional assays. In the caspase-9 functional

dx.doi.org/10.1021/jm201072x | J. Med. Chem. 2012, 55, 106–114

assay (Figure 4), XIAP protein dose-dependently inhibits the activity of caspase-9, achieving 80% of inhibition at 500 nM.

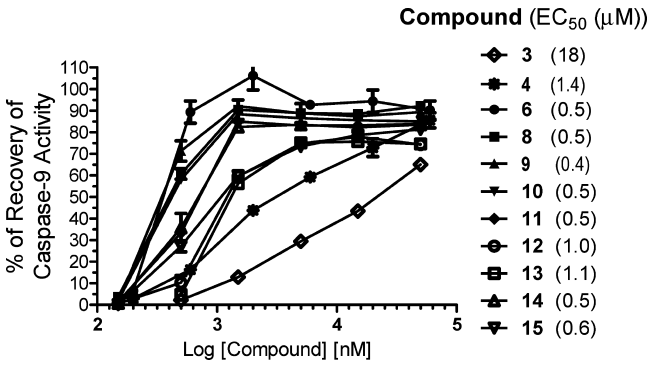

Figure 4. Smac mimetics antagonize XIAP L-BIR2-BIR3 in an in vitro caspase-9 functional assay. A 500 nM XIAP L-BIR2-BIR3 protein achieves 80% inhibition of caspase-9 activity, and Smac mimetics dose-dependently restore the activity of caspase-9. Caspase-9 activity was determined using the Z-LEHD fluorescent substrate at the 1 h time-point and was normalized to the control.

Consistent with their high binding affinities to XIAP, compounds **8**–**15** can dose-dependently antagonize XIAP to restore the activity of caspase-9, with IC_{50} of 0.5–1.0 μM, and have potencies very similar to that of our previously reported bivalent Smac mimetic **6**. The monovalent Smac mimetics **3** and **4** can also antagonize XIAP in the caspase-9 functional assay but is less potent than the bivalent Smac mimetics.

In the caspase-3 functional assay (Figure 5), XIAP protein at 20 nM can inhibit 90% of the enzymatic activity of caspase-3.

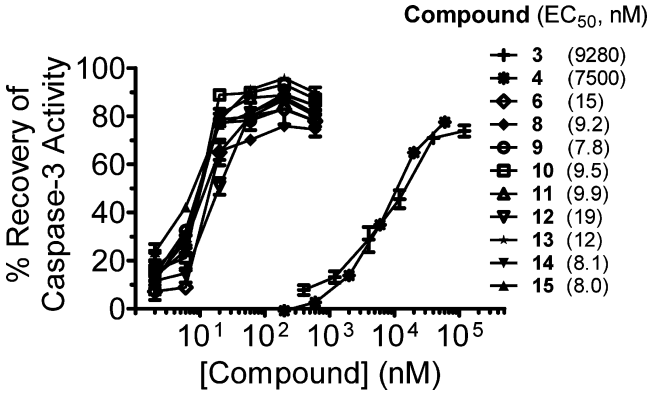

Figure 5. Smac mimetics antagonize XIAP L-BIR2-BIR3 in an in vitro caspase-3 functional assay. Recombinant XIAP L-BIR2-BIR3 protein at 20 nM inhibits caspase-3 activity by 90%. Smac mimetics dose-dependently reactivate caspase-3 activity. Caspase-3 activity was determined using the Ac-DEVD-AFC fluorescent substrate at the 1 h time-point and was normalized to the control.

All of the bivalent Smac mimetics, including compound **6**, show very similar potencies in this assay and have EC_{50} of 8–20 nM. However, the monovalent Smac mimetics **3** and **4** have weak potencies with EC_{50} values of 9.2 and 7.5 μM, respectively, and are thus >500 times less potent than the bivalent Smac mimetics. Our functional data thus show that these new bivalent Smac mimetics are highly potent in antagonizing XIAP to restore the activity of caspase-9 and caspase-3 and are >500 times more potent than monovalent Smac mimetics in the caspase-3 functional assay.

Smac mimetics can effectively inhibit cell growth in a subset of human cancer cell lines, such as the MDA-MB-231 breast cancer and SK-OV-3 ovarian cancer cell lines.[31] We tested these new bivalent Smac mimetics in cell growth inhibition assays against both the MDA-MB-231 and SK-OV-3 cancer cell lines, including **4** and **6** as controls.

In the MDA-MB-231 cell line, these new bivalent Smac mimetics inhibited cell growth with IC_{50} of 3.4–50.8 nM (Figure 6). Compounds **13** and **14** are the most potent

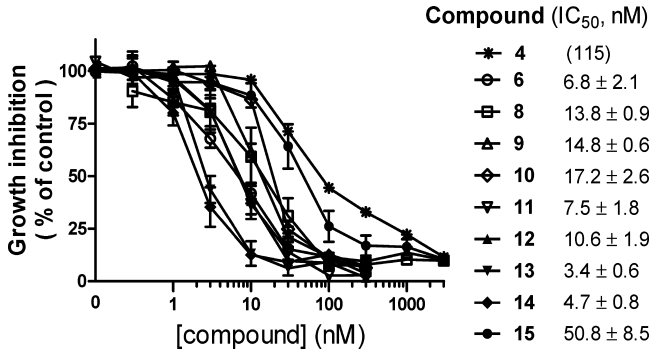

Figure 6. Inhibition of cell growth by Smac mimetics in the MDA-MB-231 human breast cancer cell line. Cells were seeded in 96-well flat-bottom cell culture plates at a density of (3–4) × 1000 cells/well and grown overnight, then incubated with Smac mimetics for 4 days. Cell growth was determined using a WST-based assay. Compounds **4** and **6** were included as control compounds.

compounds and have IC_{50} values of 3.4 and 4.7 nM, respectively, and are slightly more potent than compound **6**. Compound **15** is the least potent among these new bivalent Smac mimetics and has an IC_{50} of 50.8 nM. Since compounds **10** and **13** essentially have the same binding affinities to XIAP and cIAP1/2 proteins (Table 1), their 5-fold difference in their IC_{50} values in inhibition of cell growth is probably due to their different cell permeability, as we have demonstrated in our previous study.[38] Hence, the linker has a significant effect on the cellular growth inhibitory activity of these bivalent Smac mimetics. Of note, the monovalent control compound **4** has an IC_{50} of 115 nM and is thus >20 times less potent than compounds **13** and **14**.

In the SK-OV-3 cell line, these new bivalent Smac mimetics also effectively inhibit cell growth, with IC_{50} of 3.1–176 nM (Figure 7). Compounds **11** and **14** are the most potent with IC_{50} values of 3.1 and 4.7 nM, respectively. Compound **15** is also the least potent against the SK-OV-3 cell line. Compounds **11** and **14** are several times more potent than the bivalent control compound **6** and 50 times more potent than the monovalent control **4** in the SK-OV-3 cell line in the cell growth assay.

Mechanistic studies have shown that upon binding to cIAP1/2 in cells, Smac mimetics induce rapid degradation of cIAP1/2.[39,40] Upon cIAP1/2 degradation, Smac mimetics then induce tumor necrosis factor α (TNFα) dependent apoptosis in cancer cells that produce and secrete TNFα.[39,40] Degradation of cIAP1/2 is an essential and key early event of apoptosis induction by Smac mimetics.[39,40] To explore their cellular mechanism of action, we performed Western blot analysis of MDA-MB-231 cells treated for 24 h with bivalent mimetics **11** and **13** or the monovalent mimetic **4**, and the results are shown in Figure 8. Consistent with our previous results,[31] these compounds are potent and effective in induction of cIAP1

dx.doi.org/10.1021/jm201072x | J. Med. Chem. 2012, 55, 106–114

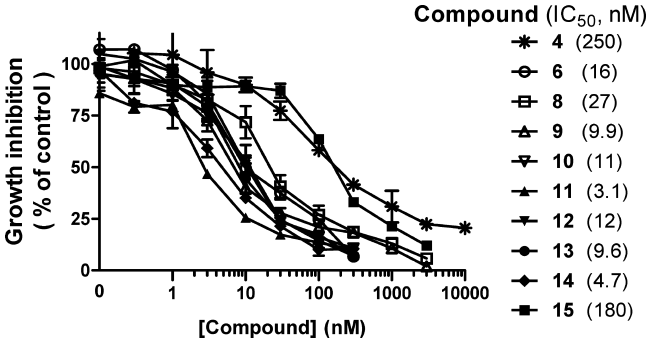

Figure 7. Inhibition of cell growth by Smac mimetics in the SK-OV-3 cancer cell line. Cells were seeded in 96-well flat-bottom cell culture plates at a density of (3−4) × 1000 cells/well and grown overnight, then incubated with Smac mimetics for 4 days. Cell growth was determined using a WST-based assay. Compounds **4** and **6** were included as control compounds.

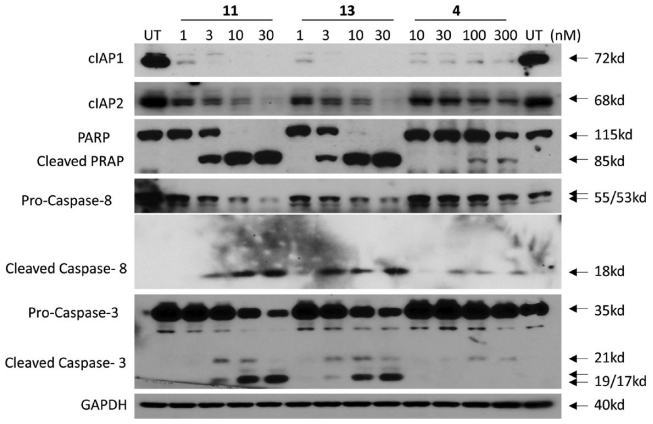

Figure 8. Western blot analysis of degradation of cIAP1 and cIAP2, cleavage of caspase-8, caspase-3, and PARP in the MDA-MB-231 cell line treated with compounds **11**, **13**, and **4** for 24 h. cIAP1, cIAP2, PARP, caspase-8, and caspase-3 were probed by specific antibodies and GAPDH was used as the loading control.

degradation. Degradation of the cIAP1 protein was essentially complete in the MDA-MB-231 cells treated with 1 nM bivalent compounds **11** and **13** or 10 nM monovalent compound **4**. These compounds also effectively induced cIAP2 degradation in a dose-dependent manner, and significant cIAP2 degradation was observed with 1−3 nM compounds **11** and **13** and 10−30 nM compound **4**. Thus, although compounds **4**, **11**, and **13** have binding affinities comparable to those of cIAP1/2 in our biochemical assays (Table 1), bivalent Smac mimetics **11** and **13** are approximately 10 times more potent than monovalent Smac mimetic **4** in induction of cIAP1/2 degradation in cells.

Compounds **11** and **13** also induced robust cleavage of casapse-8 and -3 and poly (ADP-ribose) polymerase (PARP), three key biochemical markers of apoptosis, at concentrations as low as 3 nM. Although the monovalent compound **4** can efficiently induce cIAP1 degradation at concentrations as low as 10 nM, it has a minimal effect on cleavage of caspase-8, -3, and PARP at concentrations as high as 300 nM. Similar results were obtained with these compounds in the SK-OV-3 cell line (Figure 9). Since bivalent Smac mimetics **11** and **13** are much more potent antagonists of XIAP than monovalent Smac mimetic **4**, our data further suggest that the ability of bivalent Smac mimetics to concurrently target not only cIAP1/2 but also XIAP with very high affinities is responsible for their much

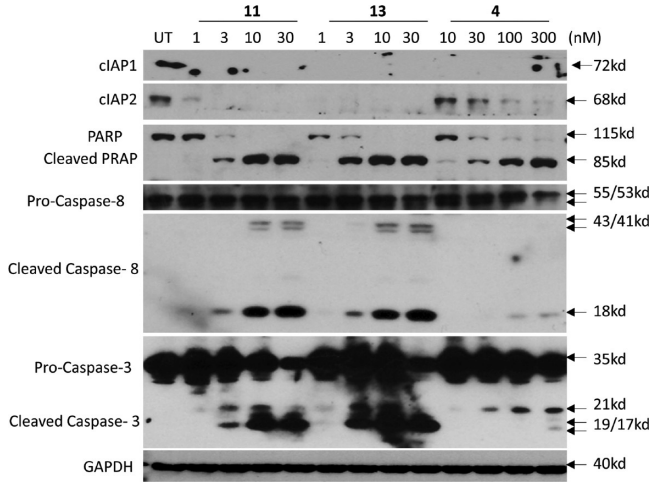

Figure 9. Western blot analysis of degradation of cIAP1 and cIAP2, cleavage of caspase-8, caspase-3, and PARP in the SK-OV-3 cell line treated with compounds **11**, **13**, and **4** for 24 h. cIAP-1, cIAP1, cIAP2, caspase-8, and caspase-3 were probed by specific antibodies and GAPDH was used as the loading control.

better anticancer activity in cell-based assays than monovalent Smac mimetics. The data for this new class of bivalent Smac mimetics are also consistent with our previous observations using a different class of bivalent compound **6** and its corresponding monovalent **1**.[31]

CONCLUSION

We have designed, synthesized, and evaluated a new class of bivalent Smac mimetics based upon a class of conformationally constrained monovalent Smac mimetics containing a diazabicyclic core structure. These new bivalent Smac mimetics (**8**−**15**) bind to XIAP, cIAP1, and cIAP2 with low nanomolar to subnanomolar affinities and function as highly potent antagonists of XIAP in functional assays. These compounds effectively induce degradation of cIAP1 and cIAP2 at concentrations as low as 1 nM in MDA-MB-231 and SK-OV-3 cancer cells and result in manifest cleavage of caspases and PARP at 3−10 nM. Consistent with the high affinities against these IAP proteins, the most potent of these compounds have IC_{50} of 3−5 nM in inhibition of cell growth in both the MDA-MB-231and SK-OV-3 cell lines. Further evaluation and optimization of these compounds can lead to the development of a new class of anticancer drugs.

EXPERIMENTAL SECTION

I. Chemistry. General Methods. ^{1}H NMR spectra were acquired at 300 MHz. ^{1}H chemical shifts are reported with $CDCl_3$ (7.27 ppm) or HDO (4.70 ppm) as internal standard. The final products were purified by C_{18} reverse phase semipreparative HPLC column with solvent A (0.1% of TFA in H_2O) and solvent B (0.1% of TFA in CH_3CN) as eluents. Purity for all the tested compounds was measured by reverse phase analytical HPLC and found to be >95%.

General Synthesis of Bivalent Smac Mimetics. *N*,*N*-Diisopropylethylamine (3 equiv) was added to a solution of compound **16** (1 equiv) and a corresponding diacyl chloride (0.55 equiv) in CH_2Cl_2. The solution was stirred at room temperature overnight and then concentrated. The residue was purified by chromatography to give a diamide. To a solution of this diamide in methanol was added HCl solution (4 N in 1,4-dioxane, 3 mL/mmol). The solution was stirred at room temperature overnight and then concentrated to yield crude product that was purified on C_{18} reverse phase semipreparative HPLC column to afford pure Smac mimetic as a salt with TFA.

dx.doi.org/10.1021/jm201072x | J. Med. Chem. 2012, 55, 106−114

(*S*,5*S*,5′*S*,8*S*,8′*S*,10a*R*,10a′*R*)-3,3′-Succinylbis(*N*-benzhydryl-5-((*S*)-2-(methylamino)propanamido)-6-oxodecahydropyrrolo-[1,2-*a*][1,5]diazocine-8-carboxamide) (8). Yield 59% over two steps. ^{1}H NMR (300 MHz, CD_3OD): 7.42−7.20 (m, 20H), 6.17 (s, 2H), 5.15 (m, 2H), 4.58 (m, 2H), 4.50−4.20 (m, 4H), 4.10−3.70 (m, 6H), 3.70−3.35 (m, 4H), 2.70 (m, 6H), 2.55−1.70 (m, 8H), 1.55 (d, J = 7.5 Hz, 6H). ESI MS: m/z 1037.6 $(M + H)^+$.

(*S*,5*S*,5′*S*,8*S*,8′*S*,10a*R*,10a′*R*)-3,3′-Adipoylbis(*N*-benzhydryl-5-((*S*)-2-(methylamino)propanamido)-6-oxodecahydropyrrolo-[1,2-*a*][1,5]diazocine-8-carboxamide) (9). Yield 62% over two steps. ^{1}H NMR (300 MHz, CD_3OD): 7.40−7.20 (m, 20H), 6.20 (s, 2H), 4.80 (m, 1H), 4.55 (m, 2H), 4.25 (m, 2H), 4.05−3.70 (m, 6H), 3.70−3.30 (m, 4H), 2.70 (s, 6H), 2.69−2.30 (m, 6H), 2.25−1.75 (m, 10H), 1.75−1.55 (m, 4H), 1.55−1.48 (m, 6H). ESI MS: m/z 1065.6 $(M + H)^+$.

(*S*,5*S*,5′*S*,8*S*,8′*S*,10a*R*,10a′*R*)-3,3′-Octanedioylbis(*N*-benzhydryl-5-((*S*)-2-(methylamino)propanamido)-6-oxodecahydropyrrolo[1,2-*a*][1,5]diazocine-8-carboxamide) (10). Yield 61% over two steps. ^{1}H NMR (300 MHz, CD_3OD): 7.45−7.20 (m, 20H), 6.15 (s, 2H), 4.80 (m, 2H), 4.55 (m, 2H), 4.25 (m, 2H), 4.05−3.80 (m, 6H), 3.80−3.30 (m, 4H), 2.70 (s, 6H), 2.70−2.25 (m, 6H), 2.20−1.75 (m, 10H), 1.75−1.50 (m, 10H), 1.50−1.30 (m, 4H). ESI MS: m/z 1093.6 $(M + H)^+$.

(*S*,5*S*,5′*S*,8*S*,8′*S*,10a*R*,10a′*R*)-3,3′-Decanedioylbis(*N*-benzhydryl-5-((*S*)-2-(methylamino)propanamido)-6-oxodecahydropyrrolo[1,2-*a*][1,5]diazocine-8-carboxamide) (11). Yield 64% over two steps. ^{1}H NMR (300 MHz, CD_3OD) δ 7.37−7.24 (m, 20H), 6.20 (s, 2H), 4.90 (m, 2H), 4.59 (m, 2H), 4.24 (m, 2H), 3.95 (m, 2H), 3.90−3.55 (m, 4H), 3.60−3.28 (m, 4H), 2.70 (s, 6H), 2.65−2.25 (m, 6H), 2.20−1.80 (m, 10H), 1.75−1.55 (m, 4H), 1.55 (d, J = 7.8 Hz, 6H), 1.45−1.25 (m, 8H). ESI MS: m/z 1121.7 $(M + H)^+$.

(*S*,5*S*,5′*S*,8*S*,8′*S*,10a*R*,10a′*R*)-3,3′-Dodecanedioylbis(*N*-benzhydryl-5-((*S*)-2-(methylamino)propanamido)-6-oxodecahydropyrrolo[1,2-*a*][1,5]diazocine-8-carboxamide) (12). Yield 63% over two steps. ^{1}H NMR (300 MHz, CD_3OD): 7.45−7.20 (m, 20H), 6.15 (s, 2H), 4.80 (m, 2H), 4.55 (m, 2H), 4.05−3.70 (m, 6H), 3.70−3.30 (m, 4H), 2.70 (s, 6H), 2.68−2.25 (m, 8H), 2.25−1.75 (m, 10H), 1.75−1.50 (m, 10H), 1.45−1.25 (m, 10H). ESI MS: m/z 1149.7 $(M + H)^+$.

(*S*,5*S*,5′*S*,8*S*,8′*S*,10a*R*,10a′*R*)-3,3′-(5,5′-(1,4-Phenylene)bis-(pentanoyl))bis(*N*-benzhydryl-5-((*S*)-2-(methylamino)-propanamido)-6-oxodecahydropyrrolo[1,2-*a*][1,5]diazocine-8-carboxamide) (13). Yield 67% over two steps. ^{1}H NMR (300 MHz, CD_3OD): 7.40−7.20 (m, 20H), 7.15−7.05 (m, 4H), 6.08 (s, 2H), 4.80 (m, 2H), 4.55 (m, 2H), 4.23 (m, 2H), 3.90 (m, 2H), 3.85 (m, 2H), 3.76 (m, 2H), 3.70−3.30 (m, 4H), 2.65 (s, 6H), 2.63−2.25 (m, 10H), 2.20−1.78 (m, 10H), 1.75−1.58 (m, 8H), 1.55 (d, J = 7.5 Hz, 6H). ESI MS: m/z 1197.7 $(M + H)^+$.

(*S*,5*S*,5′*S*,8*S*,8′*S*,10a*R*,10a′*R*)-3,3′-(5,5′-Oxybis(pentanoyl))-bis(*N*-benzhydryl-5-((*S*)-2-(methylamino)propanamido)-6-oxodecahydropyrrolo[1,2-*a*][1,5]diazocine-8-carboxamide) (14). Yield 58% over two steps. ^{1}H NMR (300 MHz, CD_3OD): 7.40−7.20 (m, 20H), 6.18 (s, 2H), 4.90 (m, 2H), 4.55 (m, 2H), 4.25 (m, 2H), 3.90 (m, 2H), 3.85−3.55 (m, 6H), 3.55−3.30 (m, 10H), 2.70 (s, 6H), 2.65−2.25 (m, 6H), 2.25−1.60 (m, 18H), 1.55 (d, J = 7.8 Hz, 6H). ESI MS: m/z 1137.6 $(M + H)^+$.

(*S*,5*S*,5′*S*,8*S*,8′*S*,10a*R*,10a′*R*)-3,3′-Terephthaloylbis(*N*-benzhydryl-5-((*S*)-2-(methylamino)propanamido)-6-oxodecahydropyrrolo[1,2-*a*][1,5]diazocine-8-carboxamide) (15). Yield 53% over two steps. ^{1}H NMR (300 MHz, CD_3OD) 7.40−7.14 (m, 24H), 6.15 (s, 2H), 5.05 (m, 2H), 4.58 (m, 2H), 4.44 (m, 2H), 3.90−3.75 (m, 6H), 3.50−3.43 (m, 4H), 2.51 (s, 6H), 2.30−1.84 (m, 12H), 1.47 (d, J = 6.9 Hz, 6H). ESI MS: m/z 1085.7 $(M + H)^+$.

II. Molecular Modeling. The crystal structure of XIAP BIR3 complexed with Smac protein (PDB entry 1G73)[16] was used to predict the binding models of XIAP BIR3 bound to designed compounds. For XIAP BIR2, the crystal structure of XIAP BIR2 complexed with caspase 3 (PDB entry 1I3O)[41] was used to predict the binding models of XIAP BIR2 bound to designed compounds. This structure was further refined through a 1 ns molecular dynamics (MD) simulation. The final XIAP BIR2 conformation at the end of 1 ns of MD simulation was used to predict the binding between AVPI and designed compounds in the docking simulations.

We used the AMBER program suite (version 8)[42] to perform the molecular dynamics (MD) simulations. The AMBER force field (ff99)[42,43] was used for the natural amino acids in the complex, and the TIP3P model[44] was used for water molecules. There is one Zn^{2+} ion covalently bound to C200, C203, H220, and C227 in the XIAP BIR2 domain. This Zn^{2+} ion, while important for structural integrity, has no direct interaction with the ligands. We used parameters developed by Ryde[45] for the Zn^{2+} ion and its coordination with the neighboring four residues to model this chelating structure in our simulation. All the MD simulations were carried out at NTP. The SHAKE algorithm[46] was used to fix the bonds involving hydrogen. The PME method[47] was used to account for long-range electrostatic interactions and the nonbonded cutoff distance was set at 10 Å. The time step was 2 fs, and the neighboring pairs list was updated after every 20 steps. For the refinement of the structure between designed compounds and the proteins, the protocol is as follows: A 500-step minimization of the solvated system was performed followed by 6 ps of MD simulation to gradually heat the system from 0 to 298 K. The system was then equilibrated by another 34 ps simulation at 298 K. Finally, the 1 ns production simulation was run and the snapshots of conformations (typically 2000), evenly spaced in time, were collected for structural analysis.

Binding poses of designed compounds with XIAP BIR2 and BIR3 were predicted using the GOLD program (version 3.1.1).[48,49] The center of the binding site was set at T308 for XIAP BIR3 and at K208 for XIAP BIR2, respectively. The radius for the binding sites was defined as 13 Å, large enough to cover the binding pocket. For each genetic algorithm (GA) run, a maximum number of 200 000 operations were performed on a population of 5 islands of 100 individuals. Operator weights for crossover, mutation, and migration were set to 95, 95, and 10, respectively. The docking simulations were terminated after 20 runs for each compound. GoldScore implemented in Gold 3.1.1 was used as the fitness function to evaluate the docked conformations. The highest ranked conformation from each of the 20 runs was saved for further analysis. The top ranked conformation from the 20 runs was taken as the predicted binding mode.

III. Fluorescence Polarization Based Assays for XIAP, cIAP1, and cIAP2 Proteins. A set of sensitive and quantitative fluorescence polarization (FP) based assays were used to determine the binding affinities of Smac mimetics to XIAP linker-BIR2-BIR3, XIAP BIR3, cIAP1 BIR3, and cIAP2 BIR3 proteins. The FP-based assay for XIAP linker-BIR2-BIR3 was described in detail previously.[30] The optimized FP-based assays using a new tracer for XIAP BIR3, cIAP1 BIR3, and cIAP2 BIRs proteins were published recently.[37]

IV. Caspase-9 and Caspase-3/7 Functional Assays. Cell-free functional assays were employed to determine the functional antagonism of our designed Smac mimetics. These assays have been described previously in detail.[38]

V. Cell Growth Inhibition Assay. The MDA-MB-231 and SK-OV-3 cell lines were purchased from the American Type Culture Collection (ATCC). Cells were seeded in 96-well flat bottom cell culture plates at a density of 3−4 × 10^3 cells/well with compounds and incubated for 4 days. The rate of cell growth inhibition after treatment with different concentrations of the inhibitors was determined by assaying with (2-(2-methoxy-4-nitrophenyl)-3-(4-nitrophenyl)-5-(2,4-disulfophenyl)-2*H*-tetrazolium monosodium salt (WST-8; Dojindo Molecular Technologies Inc., Gaithersburg, Maryland). WST-8 was added to each well to a final concentration of 10%, and then the plates were incubated at 37 °C for 2−3 h. The absorbance of the samples was measured at 450 nm using a TECAN ULTRA reader. Concentration of the compounds that inhibited cell growth by 50% (IC_{50}) was calculated by comparing absorbance in the untreated cells with that in the cells treated with the compounds.

VI. Western Blot Analysis. Cells were harvested and washed with cold PBS. Cell pellets were lysed in double lysis buffer (DLB; 50 mmol/L Tris, 150 mmol/L sodium chloride, (1 mmol/L EDTA, 0.1% SDS, and 1% NP-40) in the presence of PMSF (1 mmol/L) and protease inhibitor cocktail (Roche) for 10 min on ice, then centrifuged

at 13 000 rpm at 4 °C for 10 min. Protein concentrations were determined using a Bio-Rad protein assay kit (Bio-Rad Laboratories). Proteins were electrophoresed onto a 4−20% gradient SDS−PAGE (Invitrogen) and then transferred to PVDF membranes. After blocking in 5% milk, the membranes were incubated with a specific primary antibody, washed, and incubated with horseradish peroxidase linked secondary antibody (Amersham). The signals were visualized with a chemiluminescent HRP antibody detection reagent (Denville Scientific). When indicated, the blots were stripped and reprobed with a different antibody. Primary antibody against cleaved caspase-3 was purchased from Stressgen Biotechnologies. Primary antibodies against cIAP1 and cIAP2 were purchased from R&D systems. Primary antibody against XIAP was purchased from BD Biosciences. Primary antibodies against PARP and β-actin were purchased from Cell Signaling Technology.

AUTHOR INFORMATION

Corresponding Author

*Phone: (734) 615-0362. Fax: (734) 647-9647. E-mail: shaomeng@umich.edu.

Present Addresses

[‡]Institute of Biomedical and Health Engineering, Shenzhen Institutes of Advanced Technology, Chinese Academy of Sciences, Shenzhen, Guangdong 518055, China.

[§]Key Laboratory of Regenerative Biology and Institute of Chemical Biology, Guangzhou Institutes of Biomedicine and Health, Chinese Academy of Sciences, Guangzhou 510530, China.

[∥]ZJU-ENS Joint Laboratory of Medicinal Chemistry, Zijingang Campus, Zhejiang University, Hangzhou 310058, China.

Author Contributions

[†]These authors contribute equally.

ACKNOWLEDGMENTS

We are grateful for the financial support from the Breast Cancer Research Foundation, the National Cancer Institute, NIH (R01CA109025 and R01CA127551), the Susan G. Koman Foundation, Ascenta Therapeutics, and University of Michigan Cancer Center Core grant from the National Cancer Institute, NIH (P30CA046592). The authors thank Dr. G.W.A. Milne for his critical reading of the manuscript and many useful suggestions and Ms. Karen Kreutzer for her excellent secretarial assistance.

ABBREVIATIONS USED

IAP, inhibitor of apoptotic protein; cIAP, cellular inhibitor of apoptotic protein; XIAP, X-linked inhibitor of apoptotic protein; Smac/DIABLO, second mitochondria-derived activator of caspases or direct IAP binding protein with low pI; BIR, baculoviral inhibitor of apoptotic protein repeat; FP, fluorescence polarization; PK, pharmacokinetics; PARP, poly (ADP-ribose) polymerase; TNFα, tumor necrosis factor α

REFERENCES

(1) Nicholson, D. W. From bench to clinic with apoptosis-based therapeutic agents. *Nature* **2000**, *407*, 810−816.

(2) Ponder, B. A. Cancer genetics. *Nature* **2001**, *411*, 336−341.

(3) Lowe, S. W.; Lin, A. W. Apoptosis in cancer. *Carcinogenesis* **2000**, *21*, 485−495.

(4) Hanahan, D.; Weinberg, R .A. The hallmarks of cancer. *Cell* **2000**, *100*, 57−70.

(5) Salvesen, G. S.; Duckett, C. S. Apoptosis: IAP proteins: blocking the road to death's door. *Nat. Rev. Mol. Cell Biol.* **2002**, *3*, 401−410.

(6) Deveraux, Q. L.; Reed, J. C. IAP family proteins suppressors of apoptosis. *Genes Dev.* **1999**, *13*, 239−252.

(7) Srinivasula, S. M.; Ashwell, J. D. IAPs: What's in a name? *Mol. Cell* **2008**, *30*, 123−135.

(8) Gyrd-Hansen, M.; Meier, P. IAPs: from caspase inhibitors to modulators of NF-kappaB, inflammation and cancer. *Nat. Rev. Cancer* **2010**, *10*, 561−574.

(9) Tamm, I.; Kornblau, S. M.; Segall, H.; Krajewski, S.; Welsh, K.; Kitada, S.; Scudiero, D. A.; Tudor, G.; Qui, Y. H.; Monks, A.; Andreeff, M.; Reed, J. C. Expression and prognostic significance of IAP-family genes in human cancers and myeloid leukemias. *Clin. Cancer Res.* **2000**, *6*, 1796−1803.

(10) Vucic, D.; Fairbrother, W. J. The inhibitor of apoptosis proteins as therapeutic targets in cancer. *Clin. Cancer Res.* **2007**, *13*, 5995−6000.

(11) Hunter, A. M.; LaCasse, E. C.; Korneluk, R. G. The inhibitors of apoptosis (IAPs) as cancer targets. *Apoptosis* **2007**, *12*, 1543−1568.

(12) LaCasse, E. C.; Mahoney, D. J.; Cheung, H. H.; Plenchette, S.; Baird, S.; Korneluk, R. G. IAP-targeted therapies for cancer. *Oncogene* **2008**, *27*, 6252−6275.

(13) Fulda, S. Inhibitor of apoptosis proteins as targets for anticancer therapy. *Expert Rev. Anticancer Ther.* **2007**, *7*, 1255−1264.

(14) Du, C.; Fang, M.; Li, Y.; Li, L.; Wang, X. Smac, a mitochondrial protein that promotes cytochrome *c*-dependent caspase activation by eliminating IAP inhibition. *Cell* **2000**, *102*, 33−42.

(15) Verhagen, A. M.; Ekert, P. G.; Pakusch, M.; Silke, J.; Connolly, L. M.; Reid, G. E.; Moritz, R. L.; Simpson, R. J.; Vaux, D. L. Identification of DIABLO, a mammalian protein that promotes apoptosis by binding to and antagonizing IAP proteins. *Cell* **2000**, *102*, 43−53.

(16) Wu, G.; Chai, J.; Suber, T. L.; Wu, J. W.; Du, C.; Wang, X.; Shi, Y. Structural basis of IAP recognition by Smac/DIABLO. *Nature* **2000**, *408*, 1008−1012.

(17) Liu, Z.; Sun, C.; Olejniczak, E. T.; Meadows, R.; Betz, S. F.; Oost, T.; Herrmann, J.; Wu, J. C.; Fesik, S. W. Structural basis for binding of Smac/DIABLO to the XIAP BIR3 domain. *Nature* **2000**, *408*, 1004−1008.

(18) Shiozaki, E. N.; Shi, Y. Caspases, IAPs and Smac/DIABLO: mechanisms from structural biology. *Trends Biochem. Sci.* **2004**, *29*, 486−494.

(19) Samuel, T.; Welsh, K.; Lober, T.; Togo, S. H.; Zapata, J. M.; Reed, J. C. Distinct BIR domains of cIAP1 mediate binding to and ubiquitination of tumor necrosis factor receptor-associated factor 2 and second mitochondrial activator of caspases. *J. Biol. Chem.* **2006**, *281*, 1080−1090.

(20) Yang, Q. H.; Du, C. Smac/DIABLO selectively reduces the levels of c-IAP1 and c-IAP2 but not that of XIAP and livin in HeLa cells. *J. Biol. Chem.* **2004**, *279*, 16963−16970.

(21) Wang, S. Design of small-molecule Smac mimetics as IAP antagonists. *Curr. Top. Microbiol. Immunol.* **2011**, *348*, 89−113.

(22) Sun, H.; Nikolovska-Coleska, Z.; Yang, C.-Y.; Qian, D.; Lu, J.; Qiu, S.; Bai, L.; Peng, Y.; Cai, Q.; Wang, S. Design of small-molecule peptidic and nonpeptidic Smac mimetics. *Acc. Chem. Res.* **2008**, *41*, 1264−1277.

(23) Mannhold, R.; Fulda, S.; Carosati, E. IAP antagonists: promising candidates for cancer therapy. *Drug Discovery Today.* **2010**, *15*, 210−219.

(24) Li, L.; Thomas, R. M.; Suzuki, H.; De Brabander, J. K.; Wang, X.; Harran, P. G. A small molecule Smac mimic potentiates TRAIL- and TNF alpha-mediated cell death. *Science* **2004**, *305*, 1471−1474.

(25) Oost, T. K.; Sun, C.; Armstrong, R. C.; Al-Assaad, A. S.; Betz, S. F.; Deckwerth, T. L.; Ding, H.; Elmore, S. W.; Meadows, R. P.; Olejniczak, E. T.; Oleksijew, A.; Oltersdorf, T.; Rosenberg, S. H.; Shoemaker, A. R.; Tomaselli, K. J.; Zou, H.; Fesik, S. W. Discovery of potent antagonists of the antiapoptotic protein XIAP for the treatment of cancer. *J. Med. Chem.* **2004**, *47*, 4417−4426.

(26) Sun, H.; Nikolovska-Coleska, Z.; Yang, C.-Y.; Xu, L.; Liu, M.; Tomita, Y.; Pan, H.; Yoshioka, Y.; Krajewski, K.; Roller, P. P.; Wang, S. Structure-based design of potent, conformationally constrained smac mimetics. *J. Am. Chem. Soc.* **2004**, *126*, 16686−16697.

(27) Sun, H.; Nikolovska-Coleska, Z.; Yang, C.-Y.; Xu, L.; Tomita, Y.; Krajewski, K.; Roller, P. P.; Wang, S. Structure-based design, synthesis, and evaluation of conformationally constrained mimetics of the second mitochondria-derived activator of caspase that target the X-linked inhibitor of apoptosis protein/caspase-9 interaction site. *J. Med. Chem.* **2004**, *47*, 4147−4150.
(28) Sun, H.; Nikolovska-Coleska, Z.; Lu, J.; Qiu, S.; Yang, C.-Y.; Gao, W.; Meagher, J.; Stuckey, J.; Wang, S. Design, synthesis, and evaluation of a potent, cell-permeable, conformationally constrained second mitochondria derived activator of caspase (Smac) mimetic. *J. Med. Chem.* **2006**, *49*, 7916−7920.
(29) Zobel, K.; Wang, L.; Varfolomeev, E.; Franklin, M. C.; Elliott, L. O.; Wallweber, H. J.; Okawa, D. C.; Flygare, J. A.; Vucic, D.; Fairbrother, W. J.; Deshayes, K. Design, synthesis, and biological activity of a potent Smac mimetic that sensitizes cancer cells to apoptosis by antagonizing IAPs. *ACS Chem. Biol.* **2006**, *1*, 525−533.
(30) Sun, H.; Nikolovska-Coleska, Z.; Lu, J.; Meagher, J. L.; Yang, C.-Y.; Qiu, S.; Tomita, Y.; Ueda, Y.; Jiang, S.; Krajewski, K.; Roller, P. P.; Stuckey, J. A.; Wang, S. Design, synthesis, and characterization of a potent, nonpeptide, cell-permeable, bivalent Smac mimetic that concurrently targets both the BIR2 and BIR3 domains in XIAP. *J. Am. Chem. Soc.* **2007**, *129*, 15279−15294.
(31) Lu, J.; Bai, L.; Sun, H.; Nikolovska-Coleska, Z.; McEachern, D.; Qiu, S.; Miller, R. S.; Yi, H.; Shangary, S.; Sun, Y.; Meagher, J. L.; Stuckey, J. A.; Wang, S. SM-164: a novel, bivalent Smac mimetic that induces apoptosis and tumor regression by concurrent removal of the blockade of cIAP-1/2 and XIAP. *Cancer Res.* **2008**, *68*, 9384−9393.
(32) Sun, H.; Stuckey, J. A.; Nikolovska-Coleska, Z.; Qin, D.; Meagher, J. L.; Qiu, S.; Lu, J.; Yang, C.-Y.; Saito, N. G.; Wang, S. Structure-based design, synthesis, evaluation and crystallographic studies of conformationally constrained Smac mimetics as inhibitors of the X-linked inhibitor of apoptosis protein (XIAP). *J. Med. Chem.* **2008**, *51*, 7169−7180.
(33) Peng, Y.; Sun, H.; Nikolovska-Coleska, Z.; Qiu, S.; Yang, C.-Y.; Lu, J.; Cai, Q.; Yi, H.; Wang, S. Design, synthesis and evaluation of potent and orally bioavailable diazabicyclic Smac mimetics. *J. Med. Chem.* **2008**, *51*, 8158−8162.
(34) Zhang, B.; Nikolovska-Coleska, Z.; Zhang, Y.; Bai, L.; Qiu, S.; Yang, C.-Y.; Sun, H.; Wang, S.; Wu, Y. Design, synthesis, and evaluation of tricyclic, conformationally constrained small-molecule mimetics of second mitochondria-derived activator of caspases. *J. Med. Chem.* **2008**, *51*, 7352−7355.
(35) Sun, W.; Nikolovska-Coleska, Z.; Qin, D.; Sun, H.; Yang, C.-Y.; Bai, L.; Qiu, S.; Ma, D.; Wang, S. Design, synthesis and evaluation of potent, non-peptidic Smac mimetics. *J. Med. Chem.* **2009**, *52*, 593−596.
(36) Sun, H.; Lu, J.; Liu, L.; Yi, H.; Qiu, S.; Yang, C.-Y.; Deschamps, J. R.; Wang, S. Nonpeptidic and potent small-molecule inhibitors of cIAP-1/2 and XIAP proteins. *J. Med. Chem.* **2010**, *53*, 6361−6367.
(37) Cai, Q.; Sun, H.; Peng, Y.; Lu, J.; Nikolovska-Coleska, Z.; McEachern, D.; Liu, L.; Qiu, S.; Yang, C. Y.; Miller, R.; Yi, H.; Zhang, T.; Sun, D.; Kang, S.; Guo, M.; Leopold, L.; Yang, D.; Wang, S. A potent and orally active antagonist (SM-406/AT-406) of multiple inhibitor of apoptosis proteins (IAPs) in clinical development for cancer treatment. *J. Med. Chem.* **2011**, *54*, 2714−2726.
(38) Sun, H.; Liu, L.; Lu, J.; Bai, L.; Li, X.; Nikolovska-Coleska, Z.; McEachern, D.; Yang, C. Y.; Qiu, S.; Yi, H.; Sun, D.; Wang, S. Potent bivalent Smac mimetics: effect of the linker on binding to inhibitor of apoptosis proteins (IAPs) and anticancer activity. *J. Med. Chem.* **2011**, *54*, 3306−3318.
(39) Varfolomeev, E.; Blankenship, J. W.; Wayson, S. M.; Fedorova, A. V.; Kayagaki, N.; Garg, P.; Zobel, K.; Dynek, J. N.; Elliott, L. O.; Wallweber, H. J.; Flygare, J. A.; Fairbrother, W. J.; Deshayes, K.; Dixit, V. M.; Vucic, D. IAP antagonists induce autoubiquitination of c-IAPs, NF-kappaB activation, and TNFalpha-dependent apoptosis. *Cell* **2007**, *131*, 669−681.
(40) Vince, J. E.; Wong, W. W.; Khan, N.; Feltham, R.; Chau, D.; Ahmed, A. U.; Benetatos, C. A.; Chunduru, S. K.; Condon, S. M.; McKinlay, M.; Brink, R.; Leverkus, M.; Tergaonkar, V.; Schneider, P.; Callus, B. A.; Koentgen, F.; Vaux, D. L.; Silke, J. IAP antagonists target cIAP1 to induce TNFalpha-dependent apoptosis. *Cell* **2007**, *131*, 682−693.
(41) Riedl, S. J.; Renatus, M.; Schwarzenbacher, R.; Zhou, Q.; Sun, C.; Fesik, S. W.; Liddington, R. C.; Salvesen, G. S. Structural basis for the inhibition of caspase-3 by XIAP. *Cell* **2001**, *104*, 791−800.
(42) Case, D. A.; Darden, T. A.; Cheatham, T. E., III; Simmerling, C. L.; Wang, J.; Duke, R. E.; Luo, R.; Merz, K. M.; Wang, B.; Pearlman, D. A.; Crowley, M.; Brozell, S.; Tsui, V.; Gohlke, H.; Mongan, J. ; Hornak, V.; Cui, G.; Beroza, P.; Schafmeister, C.; Caldwell, J. W.; Ross, W. S.; Kollman, P. A. *AMBER*, version 8; University of California, San Francisco, CA, 2004.
(43) Wang, J.; Cieplak, P.; Kollman, P. A. How well does a restrained electrostatic potential (RESP) model perform in calculating conformational energies of organic and biological molecules? *J. Comput. Chem.* **2000**, *21*, 1049−1074.
(44) Jorgensen, W. L.; Chandrasekhar, J.; Madura, J. D.; Impey, R. W.; Klein, M. L. Comparison of simple potential functions for simulating liquid water. *J. Chem. Phys.* **1983**, *79*, 926−935.
(45) Ryde, U. Molecular dynamics simulations of alcohol dehydrogenase with a four- or five-coordinate catalytic zinc ion. *Proteins* **1995**, *21*, 40−56.
(46) Rychaert, J. P.; Ciccotti, G.; Berendsen, H. J. C. Numerical integration of the Cartesian equations of motion of a system with constraints: molecular dynamics of *n*-alkanes. *J. Comput. Phys.* **1977**, *23*, 327−341.
(47) Darden, T. A.; York, D. M.; Pedersen, L. Particle mesh Ewald: An $N\cdot\log(N)$ method for Ewald sums in large systems. *J. Chem. Phys.* **1993**, *98*, 10089−10092.
(48) Jones, G.; Willett, P.; Glen, R. C.; Leach, A. R.; Taylor, R. Development and validation of a genetic algorithm for flexible docking. *J. Mol. Biol.* **1997**, *267*, 727−748.
(49) Verdonk, M. L.; Cole, J. C.; Hartshorn, M. J.; Murray, C. W.; Taylor, R. D. Improved protein−ligand docking using GOLD. *Proteins* **2003**, *52*, 609−623.